Ab initio study of the annealing of vacancies and interstitials in cubic SiC: Vacancy-interstitial recombination and aggregation of carbon interstitials

Michel Bockstedte, Alexander Mattausch, and Oleg Pankratov
Lehrstuhl für Theoretische Festkörperphysik, Universität Erlangen-Nürnberg, Staudtstrasse 7 B2, D-91058 Erlangen, Germany
(Received 29 September 2003; revised manuscript received 12 January 2004; published 11 June 2004)

The annealing kinetics of mobile intrinsic defects in cubic SiC is investigated by an *ab initio* method based on density-functional theory. The interstitial-vacancy recombination, the diffusion of vacancies, and interstitials to defect sinks (e.g., surfaces or dislocations) as well as the formation of interstitial clusters are considered. The calculated migration and reaction barriers suggest a hierarchical ordering of competing annealing mechanisms. The higher mobility of carbon and silicon interstitials as compared to the vacancies drives the annealing mechanisms at lower temperatures including the vacancy-interstitial recombination and the formation of interstitial carbon clusters. These clusters act as a source of carbon interstials at elevated temperatures. In *p*-type material the transformation of the silicon vacancy into the more stable vacancy-antisite complex constitutes an annealing mechanism which is activated before the vacancy migration. Recent annealing studies of vacancy-related centers in irradiated 3C-SiC and 4H-SiC and semi-insulating 4H-SiC are interpreted in terms of the proposed hierarchy of annealing mechanisms.

DOI: 10.1103/PhysRevB.69.235202 PACS number(s): 61.72.Cc, 61.72.Ji, 66.30.−h

I. INTRODUCTION

The unique features of silicon carbide, such as the wide band gap and the electrical and thermal stability, recommend this semiconductor for high power, high-frequency, and high-temperature applications. As for any semiconductor, unwanted defects are introduced into this material by growth processes and ion implantation of dopants. Besides the primary defects—interstitials and vacancies—secondary defects such as antisites and defect clusters are created. Thermal annealing is applied to reduce these defects to an inevitable abundance. Thereby the high electron mobility is restored and the electrical activation of dopants is achieved.

The annealing properties of intrinsic and impurity-related defect centers were studied in irradiated SiC by various experimental techniques, for instance electron-spin-resonance techniques (EPR), deep level transient spectroscopy (DLTS), photoluminescence spectroscopy (PL), and positron annihilation spectroscopy (PAS). Some of the reported centers persist up to a temperature range of 1300°C–1700°C. Examples for such defects are the PL-centers D_{I} (Refs. 1–3) and D_{II} (Refs. 4,5) as well as the DLTS center Z_1/Z_2 and E_1/E_2 in 4H-SiC and 6H-SiC (Ref. 6), respectively. The microscopic origin of most of the centers is still investigated. The PL-centers $P-U$ (Ref. 7) and D_{II} have been interpreted as carbon interstitials[7] or interstitial clusters,[4] due to their carbon-related localized vibrational modes (LVM's) with frequencies above the SiC bulk spectrum. Depending on the experimental conditions some of these centers even grow in intensity during the heat treatment in a temperature range between 500°C and 1200°C, when others (e.g., vacancy-related centers) gradually vanish.[8,9,6]

Vacancies and interstitials act as diffusion vehicles for otherwise immobile point defects. Defect clusters may only be diminished by reacting with or separating into these mobile entities. Vacancy-related defects have been studied by PAS (Refs. 10–13,6) and EPR (Refs. 14–17) in irradiated material. In PAS,[10] defects related to silicon and carbon vacancies can be distinguished thanks to a considerable difference of the positron lifetimes, as predicted by theory.[18,19] EPR centers have also been identified as isolated silicon[14–16] and carbon[17,20,21] vacancies and the assignment has been verified theoretically.[15,22–24] Characteristic differences were observed for the annealing behavior of carbon and silicon vacancies in irradiated SiC. A lower annealing temperature ($\sim$500°C) was deduced for the carbon vacancy by PAS (Ref. 10) and EPR.[17] The annealing of the silicon vacancy occurs in several stages at 150°C, 350°C, and 750°C as observed by EPR (Ref. 14) in 3C-SiC in agreement with PAS (Ref. 12) data. In irradiated *n*-type 4H-SiC and 6H-SiC, however, additional annealing stages of centers related to a silicon vacancy were observed by PAS (Refs. 6,25) at temperatures up to 1450°C. This finding was explained by the formation of stable nitrogen-vacancy complexes. On the other hand, a vacancy-antisite complex was identified by EPR experiments[26] in irradiated *n*-type 6H-SiC annealed above 750°C. An EPR center with similar properties was also identified in 3C-SiC.[27] The center evolves from the silicon vacancy as a consequence of the vacancy's metastability in *p* type and intrinsic material predicted previously by theory.[28–30] In both experiments the signature of the silicon vacancy was absent. Other experiments[20,31] indicate that the carbon and silicon vacancies possess a higher thermal stability in semi-insulating than in irradiated SiC. A comprehensive interpretation of the annealing experiments in terms of simple mechanisms is lacking so far. In particular, the role that interstitials and vacancies play in the reported annealing stages is not known. Furthermore, the Fermi-level effect on the annealing behavior of the charged defects has not been clarified.

In the present paper we analyze the annealing of vacancies and interstitials in 3C-SiC at a microscopic level. We study the effect of clustering on the defect kinetics in case of carbon interstitials. An *ab initio* method within the frame-

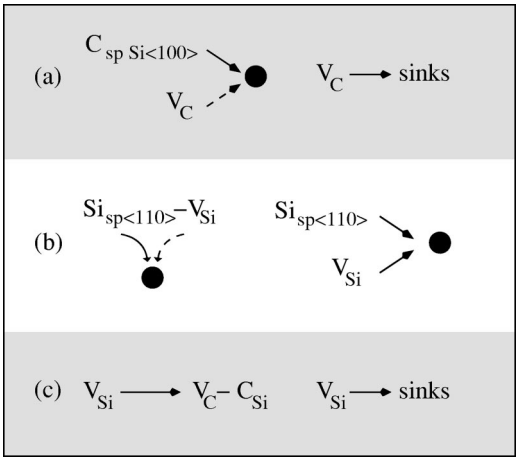

FIG. 1. Possible annealing paths of vacancies: (a) carbon vacancy: recombination of a carbon split-interstitial ($C_{sp\langle 100\rangle}$) with a carbon vacancy (V_C) and the migration of carbon vacancies to sinks, (b) silicon vacancy: Frenkel pair recombination (compensated and *n*-type material) and diffusion-limited recombination with split interstitial ($Si_{sp\langle 110\rangle}$), and (c) annealing by the metastability-induced transformation into a carbon vacancy-antisite complex (*p*-type and compensated material) and the migration of silicon vacancies to sinks (*n*-type).

work of density-functional theory (DFT) is employed to calculate the migration barriers and recombination paths. The aggregation of carbon interstititials is analyzed and the dissociation energy needed to reemit a single carbon interstitial is calculated. A hierarchy of annealing mechanisms (cf. Fig. 1) is proposed on the basis of the calculated barriers and dissociation energies under different doping conditions. For the carbon-related defects we show that the vacancy-interstitial recombination and the diffusion-limited annealing of carbon interstitials are the first two annealing stages in this hierarchy followed by the diffusion-based annealing of carbon vacancies. Besides the diffusion-limited vacancy-interstitial recombination the clustering of carbon interstitials may facilitate their annealing. Thermally stable carbon clusters reemit carbon interstitials at high temperatures thereby contributing to the kinetics of other thermally stable defects.

While the Fermi-level effect is not pronounced in the case of carbon vacancies and interstitials, it substantially affects the annealing of silicon vacancies and interstitials. This is related to the metastability of the silicon vacancy in *p*-type and intrinsic material and the existence of two different interstitial configurations in *p*-type and intrinsic or *n*-type SiC. For intrinsic (compensated) SiC, the vacancy-interstitial recombination preceeds the metastability-related transformation of the vacancy into the carbon vacancy-antisite complex, which in a next stage either dissociates or anneals via a diffusion-limited mechanism. For *p*-type conditions the transformation-induced annealing dominates over the diffusion-limited vacancy-interstitial recombination. In *n*-type material a diffusion-limited annealing of the silicon vacancy should follow the vacancy-interstitial recombination in the hierarchy of annealing mechanisms.

The outline of the paper is as follows. Preceded by a description of the method in Sec. II, we summarize the migration mechanisms of interstitials and vacancies in Sec. III. We also review the metastability of the silicon vacancy there and analyze the kinetic aspects of this metastability with emphasis on Fermi-level effects. Section IV treats the stable Frenkel pairs and the recombination paths of vacancies and interstitials. In Sec. V the properties of carbon interstitial clusters and their dissociation energies are described. The hierarchy of annealing mechanisms is outlined and discussed in the light of recent experiments in Sec. VI.

II. METHOD

We employ the plane-wave pseudopotential program package FHI96MD (Ref. 32) based on density-functional theory[33,34] and the local-density approximation[35,36] (LDA) for the exchange-correlation functional. Spin effects are included within the LSDA where noted. Defects and their environment are described using large supercells, equivalent to 64 and 216 crystal lattice sites. A special **k** point mesh[37] with 8 **k** points in the Brillouin zone ($2\times2\times2$ mesh) is used. For the description of Jahn-Teller distortions we performed the calculations in 216 atom cells at the Γ point in order to maintain the degeneracy of the defect levels. The ionization levels of charged defects were calculated following the approximate procedure proposed by Makov and Payne.[38] Optimized norm-conserving pseudopotentials of the Troullier-Martins type[39] are employed. Extensive tests showed that a basis set of plane waves with a kinetic energy up to 30 Ry yielded practically converged total-energy differences. To obtain the ground-state geometrical configuration all atoms in the simulation cell were allowed to relax.

With this *ab initio* method we analyzed the stable and metastable configurations of the vacancy-interstitial pairs and carbon clusters. All relevant charge states of the defects were included. The analysis of the defect energetics accounts for different doping conditions (characterized by the Fermi-level position μ_F) via the concept of formation energies as outlined in Ref. 30. Calculated ionization levels indicate the range of doping conditions in which a particular charge state is stable (or metastable).

Energy barriers of the vacancy-interstitial recombination were calculated taking the most stable Frenkel pairs as starting configurations and using the ridge method[40] as outlined in Ref. 30.

III. MIGRATION OF INTERSTITIALS AND VACANCIES

In this section we briefly summarize our findings for the migration of interstitials and vacancies as outlined in Ref. 30. We shall refer to these results in the following sections in the context of defect annealing.

The carbon split-interstitial $C_{sp\langle 100\rangle}$ and the carbon vacancy (V_C) migrate by second-neighbor hops on the carbon sublattice. For $C_{sp\langle 100\rangle}$ a migration between the carbon sites via the adjacent silicon sites is also possible with only slightly higher migration barriers. $C_{sp\langle 100\rangle}$ exists in positive and negative charge states, while V_C is only realized as a positive or a neutral defect in 3C-SiC due to the negative-*U* behavior[41,42,30] observed for the negative vacancy. Whether

TABLE I. Ionization levels of the mobile defects, Frenkel pairs, and carbon clusters given relative to the valence-band edge .

	$(1^+\|2^+)$	$(0\|1^+)$	$(1^-\|0)$	$(2^-\|1^-)$
V_C	1.29	1.14	2.69	2.04
V_{Si}		0.18	0.61	1.76
V_C-C_{Si}	1.24	1.79	2.19	
$Si_{sp\langle 110\rangle}$	0.4	1.1		
$C_{sp\langle 100\rangle}$	0.6	0.8	1.8	
$C_{sp\langle 100\rangle}$-V_C	0.8	1.1	1.6	
$C_{spSi\langle 100\rangle}$-$V_C$	0.4	0.7	1.8	
$Si_{TC,2}$-V_{Si}	0.5	1.2		
$Si_{sp\langle 110\rangle}$-$V_{Si}$	0.5	1.3	1.8	2.3
$(C_{sp})_2$	0.8	0.99		
$(C_{sp})_{2,tilted}$	0.7	0.8		
$(C_{sp})_3$	0.85	0.62	1.49	1.8
$(C_2)_{Hex}$-C_{sp}	0.0	0.7		
$(C_{sp})_{2,kh}$ 4H		0.10	2.78	3.13
$(C_{sp})_{2,hh}$ 4H	0.41	0.50	2.82	2.68
$(C_{sp})_{2,kk}$ 4H	0.32	0.38	2.66	2.6

V_C^{2-} may be stabilized for μ_F close to the conduction-band edge cannot be unambiguously determined. The ionization levels are listed Table I. The migration barriers of the interstitial and the vacancy depend considerably on the charge state (cf. Table II).

The migration of the silicon interstitial and vacancy strongly depends on the doping conditions. In *p*-type material, the interstitial migration is mediated by the dominating tetrahedrally carbon-coordinated interstitial (Si_{TC}^{4+}) via a kick-out mechanism. For a Fermi-level above midgap (i.e., $\mu_F > 1.1$ eV) the neutral $\langle 110\rangle$-oriented split interstitial ($Si_{sp\langle 110\rangle}$) dominates. $Si_{sp\langle 110\rangle}$ migrates by second-neighbor hops with a much lower barrier than Si_{TC}^{4+}. In case of the silicon vacancy a metastability in *p*-type or intrinsic material[26,28–30] gives rise to a strongly Fermi-level dependent kinetic behavior.[30] In *n*-type material (i.e., $\mu_F > 1.7$ eV) the negative vacancy is stable and can migrate by second-neighbor hops. However, in *p*-type or intrinsic material (i.e., $\mu_F < 1.7$ eV) the vacancy transforms into the nearest-neighbor vacancy-antisite complex V_C-C_{Si}. For the V_C-C_{Si} complex there are two choices: (a) it migrates via V_{Si} as an intermediate state or (b) it dissociates into a carbon antisite and a carbon vacancy.

TABLE II. Energy barriers for the Frenkel pair recombination in comparison with the migration barriers of vacancies and interstitials and the transformation of V_{Si} into V_C-C_{Si}.

Path	Energy barriers (eV)					
	4^+	2^+	1^+	0	1^-	2^-
$C_{sp\langle 100\rangle}$-$V_C \rightarrow \bigcirc$		1.0	0.5	0.4		
$C_{spSi\langle 100\rangle}$-$V_C \rightarrow \bigcirc$		1.2	1.2	1.4		
$Si_{TC,2}$-$V_{Si} \rightarrow C_{Si}$-$Si_C$			3.2	3.2		
$Si_{sp}\langle 110\rangle$-$V_{Si} \rightarrow \bigcirc$		0.0	~ 0.2	0.2		
$C_{sp\langle 100\rangle} \rightarrow C_{sp\langle 100\rangle}$		1.4	0.9	0.5	0.6	
$Si_{TC} \rightarrow Si_{TC}$	3.5					
$Si_{sp110\rangle} \rightarrow Si_{sp}110\rangle$				1.4		
$V_C \rightarrow V_C$		5.2	4.1	3.5		
$V_{Si} \rightarrow V_{Si}$			3.6	3.4	3.2	2.4
$V_{Si} \rightarrow V_C$-C_{Si}			1.9	2.4	2.5	2.7
V_C-$C_{Si} \rightarrow V_{Si}$		6.1	4.2	3.5	2.4	

Regarding the migration of V_C-C_{Si} we briefly outline a point that has not been considered in detail in Ref. 30. This migration is a complex interplay between the transformations V_C-$C_{Si} \rightarrow V_{Si}$ and $V_{Si} \rightarrow V_C$-C_{Si}, and the migration of V_{Si}. Note that (a) the transformation barrier V_C-$C_{Si} \rightarrow V_{Si}$ varies by almost 4 eV with the charge state and (b) the charge state is due to change along the migration path as V_{Si} and V_C-C_{Si} prefer different charge states for a given Fermi level. Provided that all involved migration events are thermally activated, the effective migration barrier is given by the formation energy difference of V_C-C_{Si} and V_{Si} for a given Fermi level and the migration barrier of the vacancy. The value for the effective migration barrier varies between 7.7 eV in *p*-type material and 3.2 eV at $\mu_F = 1.76$ eV. For a mid gap Fermi level we obtain 4.3 eV. The dissociation barrier of V_C-C_{Si} was estimated to 6.2 eV for $(V_C\text{-}C_{Si})^{2+}$ and 4.5 eV for $(V_C\text{-}C_{Si})^0$.

IV. RECOMBINATION OF FRENKEL PAIRS

A. Carbon vacancies

In a carbon Frenkel pair the interstitial and the vacancy may be either nearest neighbors or second neighbors. Vacancies and interstitials may attract each other also at larger distances. The recombination of the remote vacancy and interstitial involves a migration of the interstitial to the vacancy. In the following we analyze the recombination of Frenkel pairs with a carbon split interstitial being a nearest or a second neighbor of the carbon vacancy.

The nearest-neighbor pair $C_{spSi\langle 100\rangle}$-$V_C$ is a vacancy complex with a carbon split interstitial at a silicon site. Two different configurations are possible: a stable configuration with a three-fold coordinated carbon interstitial and a silicon dangling bond as depicted in Fig 2(a), and another configuration in which the carbon interstitial possesses one carbon neighbor. This latter pair turned out to be unstable. The first configuration exists in the charge states 2^+ through 1^-. The corresponding ionization levels are given in Table I. The negative charge state is relevant only in *n*-type material. The defect states are formed by a silicon *p* orbital of the interstitial and the silicon dangling bond of the vacancy located within the same plane. Using the saddle-point search method and a 64 atom cell with special *k* points we obtained a recombination barrier for the neutral charge state of 1.4 eV (cf Table II). At the transition state the occupied defect levels are well localized. Towards the end of the recombination they transform into delocalized valence-band states. The pair may also recombine in the positive charge states. There we expect the neutralization by an electron transfer at the end of the recombination. In this case a recombination barrier can be calculated and we obtain 1.2 eV for $(C_{spSi\langle 100\rangle}\text{-}V_C)^{2+}$ and $(C_{spSi\langle 100\rangle}\text{-}V_C)^{1+}$. For $(C_{spSi\langle 100\rangle}\text{-}V_C)^-$, which is relevant in

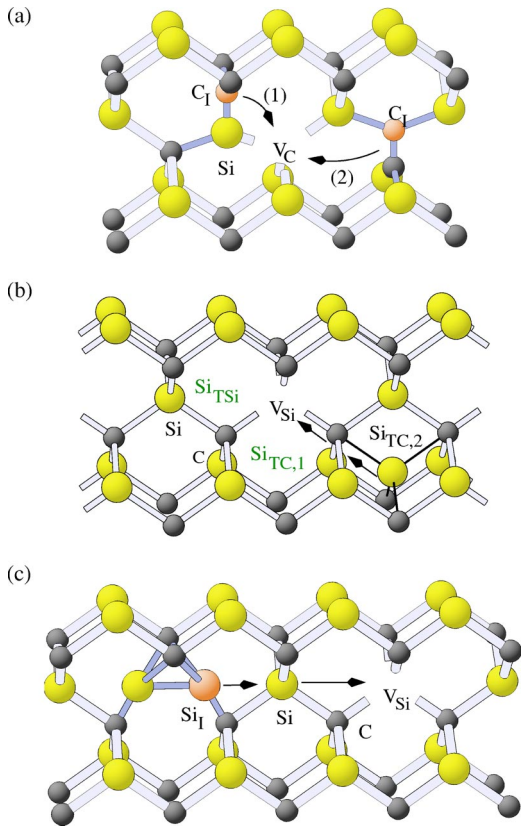

FIG. 2. Recombination of carbon and silicon Frenkel pairs: (a) carbon nearest-neighbor pair $C_{spSi\langle 100\rangle}$-$V_C$ and second-neighbor pair $C_{sp\langle 100\rangle}$-V_C, (b) silicon Frenkel pairs with Si_{TC}-interstitial (the labels Si_{TSi} and $Si_{TC,1}$ indicate the unstable sites), and (c) fourth-neighbor pair $Si_{sp\langle 110\rangle}$-$V_{Si}$. The lowest energetic path of the interstitial atom is indicated by arrows.

n-type material, a second defect level is occupied that transforms into a delocalized conduction-band state during the recombination. Two possibilities exist in this case: first, the defect is converted to neutral by an electron transfer before the recombination or second, in the final stage of the recombination the additional electron is donated into the conduction band. The treatment of both cases is beyond the scope of the present work. However, in both cases an additional energy barrier has to account for the charge-transfer process. This will hinder the recombination process in *n*-type material.

In the second-neighbor pair $C_{sp\langle 100\rangle}$-V_C the interstitial is located at the neighboring carbon site, as depicted in Fig. 2(a). The pair exists in the charge states 2^+, 1^+, 0 and 1^- (cf. Table I for the ionization levels). The defect states mainly derive from the interstitial levels. The recombination occurs by a second-neighbor hop of the upper carbon atom via the unstable $C_{spSi\langle 100\rangle}$ configuration as indicated in Fig. 2(a). The recombination barriers for the pair are listed in Table II. With values between 1.0 eV and 0.4 eV they are considerably lower than the barriers for the recombination of $C_{spSi\langle 100\rangle}$-$V_C$. The barrier is also lower than the migration barrier of the split interstitials. For the negative charge state a similar mechanism as for the negative nearest-neighbor pair has to be considered.

In *p*-type material both the vacancy and the approaching interstitial may be positively charged. An additional long-range Coulomb repulsion may hinder the recombination. The barrier for the formation of the Frenkel pair is then given by the migration barrier of the interstitial plus the Coulomb repulsion of the pair. On the other hand, once the defect levels begin to overlap the new bonding states are formed. The charge state will be successively reduced by electron transfer from the Fermi level to the defect levels. Indeed, for the Frenkel pairs discussed above the total charge of the isolated defects $C^{2+}_{sp\langle 100\rangle}$ and V_C^{2+} is reduced to 2^+ or 1^+.

A considerable energy gain is associated with the formation of the Frenkel pairs $C_{spSi\langle 100\rangle}$-$V_C$ and $C_{sp\langle 100\rangle}$-V_C from the isolated defects $C_{sp\langle 100\rangle}$ and V_C. The binding energy for $C_{spSi\langle 100\rangle}$-$V_C$ varies between 2 eV for $(C_{spSi\langle 100\rangle}\text{-}V_C)^{2+} \rightarrow C^0_{sp\langle 100\rangle} + V_C^{2+}$ and 4 eV for $(C_{spSi\langle 100\rangle}\text{-}V_C)^0 \rightarrow C^0_{sp\langle 100\rangle} + V_C^0$. For the second-neighbor pair $C_{sp\langle 100\rangle}$-V_C we obtain values between 0.8 eV for $(C_{sp\langle 100\rangle}\text{-}V_C)^{2+} \rightarrow C^0_{sp\langle 100\rangle} + V_C^{2+}$ and 1.0 eV for the separation of the neutral pair. The interstitial is thus attracted by the vacancy once the charge state has equilibrated.

Rauls *et al.*[43] investigated the recombination of vacancies with carbon split interstitials in 4H-SiC using a DFT-based tight-binding scheme. Only neutral Frenkel pairs were considered. A similar recombination barrier of the neutral pair $C_{sp\langle 100\rangle}$-V_C (0.5 eV) was found as in our calculation for 3C-SiC. Larger barriers were obtained for the direct recombination of more remote pairs. In a very recent paper[44] Gao and Weber studied the recombination of Frenkel pairs produced by low-energy recoils using classical molecular dynamics and semi-empirical Tersoff potentials. Most of the carbon interstitials created in the recoil cascade were separated only by a short distance from the vacancy. The simulations yielded activation energies between 0.24 eV and 1.6 eV for the recombination of the neutral pairs, in agreement with the results of the present work. However, some of the interstitial configurations (e.g., the tetrahedral Si-coordinated interstitial) found using Tersoff potentials are unstable in our *ab initio* calculations.

B. Silicon vacancies

Frenkel pairs involving the silicon vacancy may be formed with either of the dominant interstitials Si_{TC}, $Si_{sp\langle 110\rangle}$, and with the silicon-coordinated interstitial Si_{TSi}. The Frenkel pairs with Si_{TC} and Si_{TSi} should account for a recombination in *p*-type material, when the Si_{TC} site is relevant for the migration. A recombination via the Frenkel pair with $Si_{sp\langle 110\rangle}$ should be relevant in intrinsic (compensated) and n-type material, where split-interstitials dominate.

First we have analyzed the Frenkel pairs of Si_{TSi} or Si_{TC} interstitials with a neighboring silicon vacancy. The Frenkel pairs with a Si_{TC} interstitial or a Si_{TSi} interstitial directly next to the vacancy turned out to be unstable in all relevant charge states [the labels $Si_{TC,1}$ and Si_{TSi} refers to these interstitial sites in Fig. 2(b)]. Upon reaching these sites, the interstitial immediately recombines with the vacancy. The closest stable Frenkel pair we found involves an interstitial at a Si_{TC} site

with only one common carbon neighbor to the vacancy [c.f. the $Si_{TC,2}$ site in Fig. 2(b)]. This Frenkel pair has deep levels in the band gap. It exists only in the positive and neutral charge states (cf. Table I). The recombination of this pair could be achieved via a hop of the interstitial passing close to the adjacent Si_{TSi} site. Our calculations indicate, however, that this is not a likely path. Instead, an antistructure pair forms by a hop of the carbon neighbor into the silicon vacancy. Simultaneously, in a concerted motion, the interstitial moves into the site left by the carbon atom. The reaction barrier amounts to 3.2 eV for the positive and the neutral Frenkel pair, which is comparable with the migration barrier of Si_{TC}. In a recent molecular-dynamics simulation of Gao and Weber[44] the Frenkel pair $Si_{TC,2}$-V_{Si} was not generated by the low-energy recoil. A likely explanation is that the $Si_{TC,2}$ site is shielded by the neighboring C atom and the knocked out Si atom leaves the site in other directions with a much higher probability. However, this site should be important for the diffusion-based recombination in *p*-type material whereas in compensated and *n*-type material the interstitial may not reach this site due to the different migration mechanism. In the molecular-dynamics[44] approach the neutral pair $Si_{TC,1}$-V_{Si} was found to be stable with a recombination barrier of 0.9 eV, in contrast to our *ab initio* results.

Frenkel pairs with the split interstitial $Si_{sp\langle 110\rangle}$ represent other possible configurations. It turns out that $Si_{sp\langle 110\rangle}$-$V_{Si}$ is unstable when the vacancy and the interstitial are second neighbors, irrespective of the orientation of the pair. An immediate recombination with the vacancy occurs, and other stable configurations along the relaxation path like a split-interstitial configuration at the neighboring carbon site ($Si_{spC\langle 100\rangle}$ site) are not found. A recombination barrier thus may be encountered only for more distant pairs, e.g., with the interstitial at the third- or the fourth-neighbor shell. The recombination of such pairs is based on the migration of the split interstitial to an unstable second-neighbor position. Here we discuss the fourth-neighbor Frenkel pair in more detail. Our findings for this pair suggest a similar mechanism for the third-neighbor pair. The fourth-neighbor complex is stable except in a highly doped *p*-type material. In the latter case the doubly positively charged interstitial and the vacancy immediately recombine. Otherwise, the complex has a positively charge state for *p*-type and intrinsic conditions and becomes negatively charged in *n*-type SiC (cf. Table I). The saddle-point search finds the following recombination mechanism [cf. Fig. 2(c)]: the silicon interstitial jumps towards the silicon neighbor it has in common with the vacancy, and this neighbor is kicked out of its site. This silicon atom recombines with the vacancy. The process has a barrier of 0.2 eV. As the split interstitial close to the vacancy is unstable, the barrier for this process is considerably lower than the barrier for the interstitial migration. Regarding the recombination of the vacancy with interstitials in more distant neighbor shells, we expect that the presence of the vacancy should weaken the bonding of the interstial and hence should reduce the migration barrier of split interstitials. This means that the activation energy for the recombination varies between 0.2 eV and 1.4 eV. As discussed for the annealing of carbon vacancies, we expect a higher barrier for the recombination in the negative charge state of the complex.

TABLE III. Dissociation energy of neutral interstitial and vacancy clusters. For the interstitial clusters the given value is the energy needed to remove a single carbon atom (where Hex refers to the hexagonal configuration).

Polytype	Defect	Dissociation energy (eV)		
3C	$(C_I)_2$	4.8 (Hex)	2.8 (sp)	1.9 (tilted)
3C	$(C_I)_3$	0.4 (Hex)	3.0 (sp)	
3C	$(C_I)_4$	3.9 (Hex)	5.7 (sp)	
4H	$(C_I)_2$	5.4 (kh)	4.6 (hh)	4.6 (kk)
3C	V_C-V_{Si}		4.5	
3C	V_C-V_C		1.7	
3C	V_{Si}-V_{Si}		0.1	

Our analysis of the silicon Frenkel pairs shows that the pairs with a short distance between the interstitial and the vacancy are unstable, except for the second-neighbor pair V_{Si}-$Si_{TC,2}$. For the stable pairs we have found recombination barriers somewhat lower than the migration barriers of the relevant interstitial. The findings indicate that the recombination barriers of the interstitial with the vacancy over a larger separation does not exceed the migration barrier of the corresponding interstitial.

V. CLUSTERING OF CARBON INTERSTITIALS

A formation of composite defects, e.g., D_I or D_{II} centers, during annealing requires a reservoir of intrinsic defects. At elevated temperatures, when vacancies and interstitials anneal out (see discussion in Sec. VI), the point defects can be supplied by defect precipitations. For example, clusters of vacancies and interstitials can serve as sources of mobile defects. We expect that interstitial clusters have a much more pronounced effect on the defect kinetics than the vacancy clusters. Although both cluster types possess sizeable dissociation energies (cf. Table III and Ref. 45 for the divacancy), the migration barriers of the carbon and the silicon vacancies are much higher than those of the interstitials (cf. Sec. III) so that it is much more likely that the interstitials combine into precipitates. In addition, we expect (cf. Sec. VI) that the vacancy-interstitial recombination sets in before a significant vacancy clustering occurs.

In this section we consider small clusters of up to four carbon interstitials. Due to the high mobility of the carbon interstitials, these clusters should act as sinks for interstitials at lower temperatures and can reemit them at higher temperatures. Similar aggregates have already been investigated in diamond.[46] In SiC only carbon di-interstitials[47] and clusters at carbon antisites[48,47] have been discussed so far.

The microscopic structure of the considered carbon interstitial aggregates is displayed in Fig. 3 for 3C-SiC, an example of the di-interstitial in 4H-SiC is shown in Fig. 4. A detailed analysis of the defects and their vibrational spectra is given elsewhere.[49] Here we summarize the facts that are important for the annealing mechanisms. The focus is on the dissociation energies of these defects, i.e., the energy needed

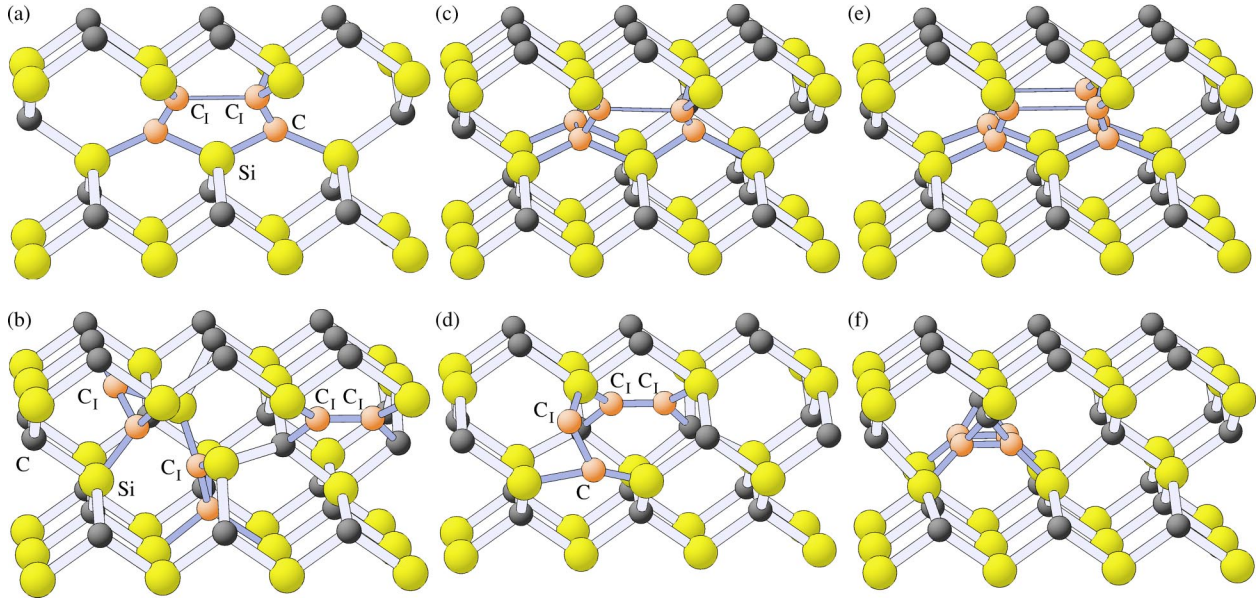

FIG. 3. Carbon interstitial clusters in 3C-SiC. Di-interstitials: (a) $(C_{sp})_2$, (b) $(C_{sp})_{2,tilted}$, and $(C_2)_{Hex}$. Tri-interstitials: (c) $(C_{sp})_3$ and (d) $(C_2)_{Hex}$-C_{sp}. Tetrainterstitials: (e) $(C_{sp})_4$ and (f) $[(C_2)_{Hex}]_2$.

to remove a single carbon atom from these clusters. For a midgap Fermi-level position all clusters are neutral. The results for the dissociation energy in the neutral charge state are listed in Table III.

The carbon split-interstitial possesses two dangling *p* orbitals oriented in ⟨110⟩ direction, resulting from the sp^2 hybridization of the carbon atoms. The two adjacent split interstitials form a covalent bond due to the overlap of these orbitals. This results in a more favorable sp^3 hybridization of the two interstitial carbon atoms [cf. Fig. 3(a)] and gives rise to a substantial energy gain. Different configurations of such a di-interstitial may exist. Three basic configurations are depicted in Figs. 3(a) and 3(b). In the configuration $(C_{sp})_2$, two of the carbon atoms form a long bond by a rotation of the interstitial dumbbells towards each other. This is associated with an energy gain of 2.8 eV. A second more stable configuration is the $(C_2)_{Hex}$ di-interstitial. In this configuration the two interstitial carbon atoms are located within a hexagonal ring and bind to the neighboring carbon and silicon atoms [cf. Fig. 3(b) right], which results in a rebonding of the hexagonal ring and an energy gain of 4.8 eV with respect to the tilted split-interstitial. The di-interstitial $(C_2)_{Hex}$ may be viewed as a reconstruction of the $(C_{sp})_2$ configuration. This was already pointed out by Gali *et al.*[47] who obtained a dissociation energy of 5.3 eV due to a different reference configuration for the split interstitial (the term bond-centered di-interstitial was used there). Further di-interstitial configurations are obtained when the two dumbbells are not contained in the {110} plane defined by the adjacent carbon sites. A complex reconstruction of the carbon-silicon bonds surrounding the dumbbell occurs as depicted in Fig. 3(b) left. This di-interstitial $(C_{sp})_{2,tilted}$ is less stable than $(C_2)_{Hex}$ and $(C_{sp})_2$. Only an energy of 1.9 eV is needed to remove a carbon atom from this structure.

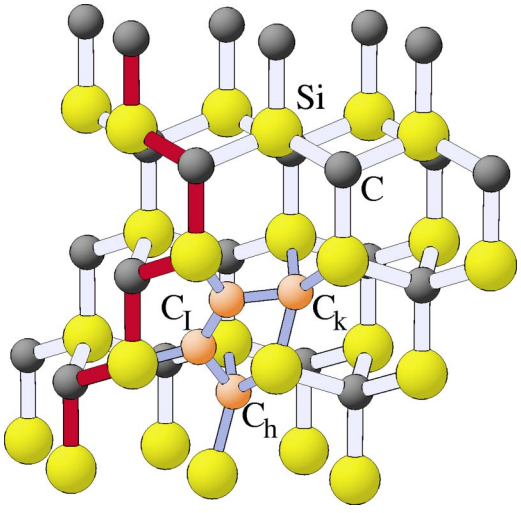

FIG. 4. Di-interstitial $(C_{sp})_{2,kh}$ in 4H-SiC located on a cubic and a hexagonal site. The subscripts *k* and *h* refer to cubic and hexagonal sites. C_I refers to the additional carbon atoms. The stacking sequence of the crystal is indicated by the dark bonds.

From the above description of the different di-interstitials it is clear that their kinetic formation depends on the migration path along which the interstitials approach each other and on the mutual orientation of the dumbbells. A reconstruction of $(C_{sp})_{2,tilted}$ into the more stable di-interstitials $(C_{sp})_2$ or $(C_2)_{Hex}$ is possible. We expect a sizable energy barrier for this process, since it involves a breaking of two carbon-silicon bonds.

The di-interstitials may act as a condensation center for larger interstitial clusters. In the same way as the di-interstitial $(C_{sp})_2$ is formed, further carbon atoms can be absorbed. The tri-interstitial $(C_{sp})_3$ [Fig. 3(c)] possesses a similar dissociation energy of 3.0 eV. In the tetrainterstitial $(C_{sp})_4$ a ring of split interstitials is formed [Fig. 3(e)] which is es-

pecially favorable. All carbon atoms are sp^3 hybrids, hence all bonds are saturated. This leads to an energy of 5.7 eV for the last added carbon interstitial. Interstitial aggregates may also grow with the hexagonal di-interstitial $(C_2)_{Hex}$ as a nucleus. A tri-interstitial based on this defect with an additional carbon interstitial as shown in Fig. 3(d) is, however, only weakly bound (0.4 eV). The reason for this weaker bonding are the less pronounced dangling *p* orbitals for the structure located in the hexagonal ring. With the addition of another split interstitial a tetrainterstitial $[(C_2)_{Hex}]_2$ is formed after some reconstruction [cf. Fig. 3(f)]. A dissociation energy of 3.9 eV $[(C_2)_{Hex}]_2$ is needed to remove the additional carbon atom.

The charge states of the investigated clusters are listed in Table I. The di-interstitial $(C_{sp})_2$ possesses all charge states from $2+$ through 0, whereas the hexagonal di-interstitial $(C_2)_{Hex}$ is neutral for all values of the Fermi level. The tri-interstitials $(C_{sp})_3$ is mainly neutral, only at the band edges the charge states $2+$ and $2-$ can exist. This cluster exhibits a negative-*U* effect, since it is energetically favorable to fully occupy the connecting bonds between all three adjacent split interstitials [cf. Fig. 3(c)]. The tetrainterstitials $(C_{sp})_4$ and $[(C_2)_{Hex}]_2$ are electrically inactive, since all carbon *p* orbitals are saturated.

In 4H-SiC, many more types of di-interstitials can exist due to the inequivalent cubic and hexagonal lattice sites. We have considered three different versions of the di-interstitial that either lie completely in a hexagonal or a cubic plane or occupy two adjacent cubic and hexagonal sites. The structure of the latter is displayed in Fig. 4, an inequivalent structure involving the other adjacent hexagonal site is also possible. With a dissociation energy of 5.4 eV the *kh* structure is the most stable of the investigated configurations. Also the purely hexagonal and cubic di-interstitials are very stable with a binding energy of 4.6 eV. These di-interstitials cause a strong lattice distortion and have a nearly linear structure within their cubic or hexagonal plane. As in 3C-SiC it is possible for these clusters to grow. Since for the hexagonal di-interstitial in 3C-SiC the bonds are strong, the dissociation energy for an additional carbon atom (about 1.2 eV for the hexagonal-cubic-hexagonal tri-interstitial) is much lower than that of the di-interstitial itself.

The microclusters presented in this section are only few examples of the clustering processes. The formation of cluster networks via bonds between the *p* orbitals of adjacent $(C_{sp})_2$ and $(C_{sp})_3$ clusters is also possible. Additionally, carbon antisites can trap carbon interstitials with sizable binding energies.[50] In the following, we outline the competition of the cluster formation with the vacancy-interstitial recombination and the role of clusters as sources of carbon interstitials at the high-temperature annealing.

VI. HIERARCHY OF ANNEALING MECHANISMS

The annealing of vacancies and interstitials is governed by several competing mechanisms. The principal mechanisms are (i) the recombination of vacancies and interstitials, (ii) the out-diffusion to the surface, (iii) the diffusion to sinks, where they annihilate or form stable complexes, and (iv) the transformation of metastable (under certain conditions) point defects into other more stable complexes. Sinks for interstitials or vacancies could be immobile defects, such as interstitial clusters and stable complexes with impurities, or extended defects, such as dislocations. In the latter cases the interstitial or vacancy do not disappear as such, but are bound in a more stable form. In the experiment, nevertheless, the observed signatures *anneal out*, while other centers related to the annealing may appear in the spectra.

The experimental investigation of the annealing kinetics requires a sufficient temperature *T* to activate one or more of the annealing mechanisms. The diffusion-limited mechanisms (ii) and (iii), and the transformation-related mechanisms are typically described by first-order kinetics with an activation energy given by the migration or transformation barrier (e.g., Ref. 51). The kinetics of the vacancy-interstitial recombination depends on the average separation of the vacancy and interstitial. For bound Frenkel pairs the activation energy is given by the recombination barrier. For uncorrelated vacancy-interstitial pairs (i.e. when the separation is much larger than the capture radius) the interstitial has to migrate to the vacancy (which is rather immobile) to form a Frenkel pair. The Frenkel pair then recombines by a hop of the interstitial into the vacant lattice site. In this case, as the recombination barriers of the Frenkel pair are found to be relatively small, the recombination is essentially limited by the diffusion of the interstitial. The recombination then is described by the activation energy of the interstitial migration. The prefactors of the diffusion-limited mechanisms and the vacancy-interstitial recombination depend on parameters of the sample preparation, e.g., the average distribution (and concentration) of the defects (and sinks), as well as the mutual interaction between the involved partners. Hence, the predictive translation of activation energies into annealing temperatures hinges on parameters that are specific to the particular samples. Only by detailed simulations it is possible to assess the initial state of the samples (e.g., after irradiation) and the annealing kinetics quantitatively. Our analysis forms the basis for such simulations that are beyond the scope of the present paper. Nevertheless, a qualitative assessment of the kinetics via the calculated activation energies should be valid, since the activation energies differ substantially in value and enter the rate constants exponentially.

In the next sections we deduce a hierarchy of annealing mechanisms for vacancies and interstitials from a comparison of the energy barriers. Consequences of this hierarchy for the annealing of ion-implantation induced damage are briefly discussed.

A. Silicon vacancies and interstitials

Qualitatively, the annealing of silicon vacancies is subject to three different Fermi-level dependent mechanisms: (i) the transformation of the silicon vacancy into a carbon vacancy-antisite complex, (ii) the Frenkel pair recombination with silicon split interstitials, and (iii) the migration of silicon vacancies to sinks. These mechanisms are summarized in Fig. 1.

In *p*-type material, we expect a dominance of the annealing of the vacancy signature by its transformation into the

vacancy-antisite complex. The recombination of the stable Frenkel pairs, i.e., the pairs with the Si_{TC} interstitial located in the second-neighbor shell or beyond, is suppressed by the larger migration/recombination barrier (3.2 eV–3.5 eV) as compared to the barrier of the transformation (1.9 eV–2.4 eV). Also the migration of the silicon vacancy is suppressed in *p*-type material due to the large migration barrier (3.6 eV–3.2 eV). Once the silicon vacancy is transformed into the vacancy-antisite complex, it stays in this configuration. The reverse transformation requires a fairly high temperature due to the large barrier of 6.5 eV. As outlined in Sec. III, the dissociation of the vacancy-antisite complex becomes possible at the same time.

In compensated material (with the Fermi level at or above midgap), the silicon split interstitial is the most relevant interstitial configuration. Its migration barrier is lower than the transformation barrier of the silicon vacancy. Hence the vacancy-interstitial recombination prevails in the annealing hierarchy. For the recombination of bound Frenkel pairs we found a low barrier of 0.2 eV. The annihilation of vacancies with more distant interstitials is limited by the migration of the interstitial towards the vacancy with a migration barrier of 1.4 eV. It constitutes a separate annealing stage. Note that the small binding energy of the Frenkel pair indicates a weak attractive interaction between the interstitial and the vacancy. Hence a dissociation of distant pairs has a relatively high probability, which enables further annealing stages. The metastability-induced annealing is the next annealing stage in the hierarchy. As a final stage, the vacancy-antisite complex, that evolves from the silicon vacancy, anneals by dissociation or by its migration to sinks. Again the migration of silicon vacancies does not directly contribute as the migration barrier of 3.2 eV to 3.4 eV (V_{Si}^{-} and V_{Si}^{0} respectively) is larger than the transformation barrier.

In *n*-type material the silicon vacancy is a stable defect. As in intrinsic (compensated) material the annealing by vacancy-interstitial recombination has a lower activation barriers than the vacancy migration. The migration of silicon vacancies to sinks is most likely the last stage in the hierarchy. It has a slightly higher barrier than the transformation $V_{Si} \rightarrow V_C - C_{Si}$ in compensated material.

By electron spin-resonance experiments Itoh *et al.*[14] observed the annealing of the T1-center in *p*-type and *n*-type 3C-SiC irradiated by electrons and protons. They found three annealing stages at 150°C, 350°C and 750°C. The annealing behavior was found to be insensitive to the doping (aluminum and nitrogen) and the irradiating particles (electrons and protons), except for the *p*-type electron-irradiated sample, where the final annealing occurred at 350°C in coincidence with the annealing of three other defect centers. Itoh *et al.* argued that a possible loss of the paramagnetic state might be correlated with the annealing of two unidentified centers *T*6 and *T*7 that were only observed under these conditions.[14] The independence of the annealing behavior of the particular dopants indicates that the observed annealing process itself involves only intrinsic defects.

The *T*1 center was identified by the authors as a negative silicon vacancy V_{Si}^{-}. Later this identification was verified theoretically[15,22,23,30] by calculations of the hyperfine tensors. According to earlier theoretical results[15,41,42] and our calculations (cf. Table I) the silicon vacancy is in a negative charge state over a wide range of the Fermi level starting below midgap ($\mu_F > 0.6$ eV) and ending somewhat below the conduction-band edge ($\mu_F < 1.76$ eV). This suggests that the *p*-type and *n*-type samples were compensated by the irradiation, most likely the Fermi level was trapped by irradiation-induced deep defects around midgap. Under these conditions the scenario for compensated material we described above should explain the annealing of the EPR signature of V_{Si}^{-} by three annealing stages, namely: (i) the initial recombination of Frenkel pairs with a small separation between the vacancy and interstitial, (ii) the recombination of vacancies and interstitials with a larger separation that is limited by the diffusion of the interstitial, and (iii) the transformation of V_{Si}^{-} into a carbon vacancy-antisite complex.

From the annealing experiments Itoh *et al.*[52] deduced an activation energy of 2.2 eV for the last annealing stage. According to our calculations the transformation of V_{Si} into $V_C - C_{Si}$, that constitutes the third annealing stage, is associated with an activation energy of 2.5 eV (cf. Table II) in good agreement with the experimental result. Once this transformation is activated silicon vacancies are largely transformed into carbon vacancy-antisite complexes and the EPR signal of the *T*1-center vanishes. During the short observation times (5 min) of the isochronal annealing the reappearance of V_{Si}^{-} is kinetically hindered. Even though a signature of the carbon vacancy-antisite complex may develop in the spectra, Itoh *et al.* reportedly have not observed the appearance of a new defect center that could evolve from the silicon vacancy. Note, that for a Fermi level below 1.24 eV the vacancy-antisite complex is not paramagnetic. Only in a small window, for a Fermi level between 1.24 eV and 1.79 eV the paramagnetic positive charge state should prevail. Recently, Lingner *et al.* identified the $V_C - C_{Si}$ complex by spin-resonance experiments in neutron-irradiated *n*-type 6H-SiC.[26] The hyperfine structure of an excited high spin state ($S=1$) of this complex was detected using the magnetic dichroism of the adsorption (MCDA) and MCDA-EPR. The theoretical analysis showed that the excited state is related to an intradefect excitation of $(V_C - C_{Si})^{2+}$, which is not paramagnetic in its ground state and therefore could not be detected by standard EPR. This is consistent with the observation of Itoh *et al*. The complex appeared only in samples annealed above the temperature at which the T1-center in 3C-SiC finally vanishes. EPR centers with a similar *g* tensor and fine structure constant *D* were observed earlier in *n*-type 6H-SiC (Ref. 53) (*P*6 and P7 centers) and in electron irradiated nominally undoped 3C-SiC (*L*3 center).[27] The similarity suggests that the carbon vacancy-antisite complex as a common model for all these centers. Indeed, the annealing study of Son *et al.* shows that the center appears only after an annealing at 700°C–750°C. These observation support our interpretation of the annealing stages for the silicon vacancy reported by Itoh *et al.* An diffusion-based annealing mechanism, that was proposed earlier,[14,27] is apparently not involved in these experiments.

Using PAS Kawasuso *et al.*[10,12] have observed the annealing of vacancy-related defects in electron-irradiated *n*-type 3C-SiC and 6H-SiC. Two lifetime components were extracted from the positron signal in 6H-SiC. One component was attributed to defects related to silicon vacancies.[18,19] The other was shown to originate from carbon vacancy-related defects. In 3C-SiC only the component corresponding to silicon vacancy-related defects was detected. Kawasuso *et al.* found that this lifetime component annealed in several stages. For annealing temperatures below 500°C two annealing stages were observed in 3C-SiC and 6H-SiC that followed the findings for the T1-center in 3C-SiC. In 3C-SiC vacancy-related defects were not detected above the annealing temperature of the $T1$ center. This finding is also consistent with our interpretation of the annealing stages, since a positive carbon vacancy-antisite complex would repel the positron and therefore should not contribute to the positron lifetime.

In 6H-SiC, however, the signal persisted the annealing at 750 °C and finally annealed at 1450 °C. Yet, an annealing stage with a less pronounced drop of the vacancy concentration is present at 750 °C. In a more recent PAS study[6] using electron irradiated *n*-type 6H-SiC Kawasuso *et al.* describes the annealing of the silicon vacancy or related defect complexes with the a major stages at 500 °C–700 °C and 1000 °C–1200 °C. The vacancy signature reached the bulk level at 1200 °C. In comparison to this more recent study, the samples of the earlier study had a larger nitrogen concentration (carrier density of 5.5×10^{17} cm^{-3} at room temperature vs 5×10^{15} cm^{-3}) and were irradiated with more energetic electrons at a lower dose ($1\times10^{17}\,e^{-}$/cm^2 at 3 MeV compared to $3\times10^{17}\,e^{-}$/cm^2 at 2 MeV). The differences in the annealing behavior is most likely related to these variation in the nitrogen concentrations and the irradiation conditions.

In the following we comment on the presence of the annealing stages above 1000 °C in 6H-SiC. In their analysis of the earlier experiment Kawasuso *et al.* explained the final annealing stage at 1450 °C in terms of the dissociation of vacancy-nitrogen complexes and the subsequent annealing of the vacancy by out-diffusion or diffusion to sinks. The V_{Si}-N complexes were expected to form during the annealing. Such an interpretation is plausible as similar positron lifetimes are predicted for the V_{Si}-N complexes and the silicon vacancy.[18] Very recent theoretical investigations show that these complexes are thermally stable in agreement with EPR experiments.[54,55] Yet, also the transformation into the carbon vacancy-antisite complex may play a relevant role in the PAS experiments, provided that the sample remains compensated (Fermi level around 1.7 eV) and that the positron annihilation at the carbon vacancy-antisite complex resembles that for the silicon vacancy. Precise calculations based on *ab initio* methods for this center are lacking sofar. However, calculations[56] using an approximate method based on the superposition of atomic densities (cf. Ref. 57) using the atomic coordinates obtained for V_{C}-C_{Si} obtained in our work indicate for 4H-SiC, that the positron lifetime associated with this center lie in the range similar to the value of the silicon vacancy (at the cubic site between 162 ps to 175 ps and at the hexagonal site 187 ps to 193 ps depending on the charge state). Thus the positron lifetime does not significantly change when the negative silicon vacancy transforms into the neutral hexagonal vacancy-antisite complex. The migration of the carbon vacancy-antisite complex is associated with larger barriers than the transformation and hence is activated at higher temperatures. This scenario is a plausible explanation of the observed annealing of the V_{Si}-related signature in the PAS experiments, since the complex at the hexagonal site may become neutral during the annealing of compensating centers in *n*-type 4H-SiC. Obviously, Fermi-level effects are relevant. The annealing characteristics should therefore depend on the polytype (due to the different band-gap width). Based on our present understanding, we do not exclude the formation of vacancy-nitrogen complexes as an explanation of the final annealing stage. The interpretation of the last annealing stage in terms of vacancy-nitrogen complexes, however, requires that the dopant is present in similar or higher concentrations than the vacancies at the onset of the annealing stage.

B. Carbon vacancies and interstitials

For the carbon vacancy the annealing hierarchy starts with the vacancy-interstitial recombination at the first annealing stage and ends with the diffusion of vacancies to sinks or its out-diffusion (cf. Fig. 1). The recombination of Frenkel pairs containing the carbon split interstitial as the nearest or second neighbor of the vacancy proceeds with lower recombination barriers than the vacancy diffusion. Similarly the migration barrier for the carbon split interstitial is lower than for the carbon vacancy. For the vacancy-interstitial recombination, the migration of the interstitial towards the vacancy is the bottle neck, since recombination of the nearest- or second-neighbor Frenkel pairs proceeds with a similar or lower barrier. The annealing of the vacancy based on its diffusion therefore should be activated at much higher temperatures than the vacancy-interstitial recombination.

In irradiated material, where interstitials and vacancies are present in similar concentrations, we expect the vacancy-interstitial recombination to represent the first annealing stage. Our finding of a relevant binding energy for all charge states of the nearest- and second-neighbor Frenkel pair suggests an attractive interaction that traps the interstitial in the vicinity of the vacancy. Hence, we expect that a recombination of these Frenkel pairs has a higher probability than their dissociation. However, the diffusion-limited recombination of the isolated defects may be hindered by a Coulomb repulsion of the charged defects. This occurs only in *p*-type material for a Fermi level below 0.8 eV (cf. Table I). Above this value the carbon split interstitial is neutral. Even though the split interstitial becomes negative in *n*-type 3C-SiC, the vacancy should remain neutral. For *n*-type 4H-SiC, on the other hand, our calculations show that also the carbon vacancy becomes negative as a consequence of the larger band gap. The additional Coulomb barrier in *p*-type 3C-SiC and *p*-type or *n*-type 4H-SiC may leave a considerable fraction of vacancies unannealed in this first annealing stage. At the same time the carbon split interstitials could anneal by diffusion to

other defects where thermally stable defects complexes or defect clusters could be formed. The remaining vacancies anneal in a second annealing stage based on the vacancy diffusion.

So far the isolated carbon vacancy was neither detected by EPR experiments nor by PAS experiments in irradiated 3C-SiC. A spin-resonance center $T5$ was observed together with the $T1$ center (V_{Si}^{-}) by Itoh *et al.* that annealed at 150 °C. Its hyperfine (HF) signature originates from four silicon atoms and it was therefore identified as a defect on the carbon sublattice. However, the original assignment to the positive carbon vacancy had been revised to a complex of two hydrogen atoms with a carbon vacancy,[58,59] given the D_2 symmetry of the center that is incompatible with the theoretical findings[41,42] for the carbon vacancy. Based on the calculations of HF parameters for these models and the carbon split interstitial it was recently shown that only the split interstitial may explain the experimental findings for the $T5$ center.[60,24,23,61] Such an identification of the $T5$-center has to be verified experimentally, as the carbon HF tensors of the $\langle 100\rangle$-oriented carbon dumbbell have so far not been observed. Yet, this model would explain the low annealing temperature of the $T5$ center. According to our analysis the positive carbon split interstitial is indeed a highly mobile defect, with a migration barrier of only 0.9 eV. A comparison of the ionization levels of this defect and V_{Si} (cf. Table I) shows that $C_{sp\langle 100\rangle}^{+}$ and V_{Si}^{-} simultaneously exist in a paramagnetic state for a Fermi level around 0.7 eV in the *p*-type samples which is in agreement with the simultaneous observation of the $T1$ and $T5$ center.[14] At these doping conditions the carbon vacancy prevails in the nonparamagnetic doubly positive charge state. This explains why the carbon vacancy was not detected in EPR experiments or by PAS (the positron recombination at the positive vacancy is suppressed by the Coulomb repulsion). Therefore the mechanism (vacancy-interstitial recombination or other diffusion-limited mechanisms) behind the annealing of the $T5$ center cannot be deduced from the present experiments.

A competing process to the vacancy-interstitial recombination is the formation of carbon interstitial clusters as discussed in Sec. V. Most of these clusters possess high dissociation energies, hence they would emit interstitials mainly at elevated annealing temperatures. These interstitials then take part in further defect reactions. For the di-interstitial and the tri-interstitial in 3C-SiC, a dissociation energy of 3 eV plus an additional barrier, which may be approximated by the migration barrier of the interstitial (0.5 eV for $C_{sp\langle 100\rangle}^{0}$), is needed to remove a carbon atom. The total activation barrier is thus only slightly lower than the migration barrier of the carbon vacancy (4.1 eV for V_C^{+} and 3.5 eV for V_C^{0}). With dissociation barriers of 4.8 eV and 5.7 eV the hexagonal di-interstitial and the tetrainterstitial are much more stable and should emit interstitials at higher temperatures than the di- and tri-interstitial. A comparison of the dissociation energies with the activation energies of the other processes suggests that new carbon interstitials should be supplied at temperatures above 1000 °C. Indeed, the concentration of the photoluminescence centers D_I (Ref. 2) and D_{II},[4] presumably related to antisites[62,63] and carbon aggregates,[4,64] rises significantly at annealing temperatures above 1000 °C.[8,3] For both formation processes the availability of free carbon atoms is an important prerequisite.[62,64] Defects similar to the carbon clusters described here are known from other semiconductors. Besides the carbon clusters in diamond[46] one can also mention here the well known {311} defects in silicon. These defects emit silicon interstitials and thereby drive the transient enhanced diffusion of dopants during the annealing.[65]

In contrast to 3C-SiC, the signatures of the carbon vacancy and interstitial were reported in 4H-SiC. In irradiated *p*-type 4H-SiC, two EPR centers ($EI1$ with $S=1/2$ and $EI3$ with $S=1$) were recently identified by Son *et al.* (Ref. 66) that possess a similar g tensor as the $T5$ center in 3C-SiC. The analysis of the HF signature showed that the defects are located on the carbon sublattice. The calculations indicate that the observed silicon HF tensors are consistent with the theoretical values for the positive and neutral carbon split interstitial, respectively.[61,67,60] Similar to the $T5$ center the $EI1$ and $EI3$ center anneal around 200 °C. In *p*-type 4H-SiC irradiated at 400 °C Son *et al.*[17,66] observed by EPR experiments the final disappearance of the $EI5$ center at 500 °C. The center was tentatively assigned to a positive carbon vacancy. This assignment was verified by calculations of HF tensors,[22,23,67] and it was shown that the center is located at the cubic site. The low annealing temperature of the $EI5$ center is consistent with our discussion of the vacancy-interstitial recombination in 3C-SiC. The observation of this annealing stage for the carbon vacancy in the EPR experiments is also consistent with PAS experiments[10] performed in irradiated 6H-SiC. There it was found that the corresponding lifetime component annealed at 500 °C.

Recently, Konovalov *et al.*,[20] Zvanut and Konovalov,[68] and Son *et al.*[69] have studied EPR centers in semi-insulating 4H-SiC. They identified the centers $ID1$ (Refs. 20,68) and $EI5$ (Ref. 69). The latter was already observed in irradiated 4H-SiC. The center $ID1$ resembles the $EI5$ center with respect to its g tensor and HF values, which suggest a common identification as a carbon vacancy at the cubic lattice site.[24] Both centers possess a higher thermal stability than the $EI5$ center in irradiated SiC. For example Konovalov *et al.* have found that the center persists up to 850 °C.[20] The material used by Konovalov *et al.* and Zvanut and Konovalov was high purity, as-grown (0001) 4H-SiC wafers grown by the seeded sublimation method. The high temperatures (>2000 °C) applied during growth suggest that intrinsic defects are present in the material close to their equilibrium abundance. This means that carbon vacancies by far outnumber carbon interstitials, due to the much lower formation energy of the vacancy as compared to the interstitial. Also, the concentration of carbon interstitial clusters is predicted to be well below the vacancy concentration. Therefore the excess concentration of carbon vacancies in a material grown at high temperatures may reach its equilibrium concentration at lower temperature only by a mechanism based on the vacancy diffusion. The large migration barrier of the carbon vacancy—4.1 eV for V_C^{+} in 3C-SiC—explains the high thermal stability of carbon vacancies in as-grown semi-insulating

samples. This argument also applies to vacancies in irradiated material that escaped a vacancy-interstitial recombination (see also Umeda *et al.*[17]).

C. Implantation damage

In experiments on the annealing of implantation damage the implantation-induced disorder is monitored for example by Rutherford backscattering instead of the signature of individual defect centers. Attributing the annealing stages of the relative disorder to specific annealing mechanisms is hence more indirect than in the cases discussed above. Yet, the same principal mechanisms apply to the postimplantation annealing provided an amorphization did not take place. Depending on the implantation temperature, some of the annealing mechanisms may be thermally activated during the implantation and the corresponding annealing stages are absent in the consequent annealing experiment. Immediately after a low-temperature implantation the sample will be compensated. The Fermi level may relax towards the valence or conduction band only when defects compensating or passivating the dopants are annealed out.

Provided a low implantation temperature, the first annealing stages are related to the recombination of Frenkel pairs. The recombination of silicon Frenkel pairs and the diffusion-limited recombination of carbon interstitials with vacancies should occur during a first major stage. For silicon Frenkel pairs the barrier lies between 0.2 eV and 1.4 eV depending on the separation of the vacancy and the interstitial. The barrier of the carbon vacancy-interstitial recombination amounts to 0.5 eV in compensated material. A second stage will be connected with the diffusion-limited recombination of silicon interstitials and the recombination of nearest-neighbor carbon Frenkel pairs. Both processes have similar barriers in the range of 1.2–1.4 eV. Frenkel pairs of the type $Si_{TC,2}$-V_{Si} should not be created by a direct recoil or by the diffusion of Si interstitials in compensated material for reasons discussed in Sec. IV.

Antisites may be formed by a vacancy-interstitial recombination during the initial annealing stages. These defects also contribute to the observed disorder. Since carbon and silicon interstitials travel along the lattice sites in compensated material it is quite likely that they interact with antisites and annihilate (or even create) them.[62] For instance a carbon interstitial may annihilate a silicon antisite and create a silicon interstitial with a reaction barrier of 2 eV (the barrier for the creation of the antisite amounts to 3 eV) according to our calculations.

Additional annealing stages originate in the thermal dissociation of stable defect aggregates such as carbon interstitial clusters and in the activation of the vacancy diffusion. The processes have activation energies in the range between 3 eV and 6 eV (cf. Tables II and III). A general interpretation of the high-temperature annealing stages in terms of these mechanisms critically depends on the implantation parameters (dose, temperature, etc.) and on the actual dopant activation as discussed in the previous sections and is avoided here.

Recently, Zhang *et al.*[70] analyzed the annealing of 4H-SiC implanted with aluminum at 150 K using Rutherford backscattering to monitor the implantation damage. For samples implanted with low Al doses of two characteristic annealing stages were observed in the temperature ranges 250–420 K and 470–570 K. The annealing stages occurred on the carbon and the silicon sublattice. Their findings are consistent with the two annealing stages proposed by our analysis. These annealing stages may not be observable by positron annihilation as the Frenkel pairs are neutral or positive. Investigations of the dose-rate effects in 4H-SiC implanted at 80–160 °C by Kuznetsov *et al.*[71] show that a dynamic annealing during the implantation occurs with an activation energy of 1.3 eV. This activation energy is consistent with the recombination barrier of the carbon nearest-neighbor Frenkel pair and the diffusion limited recombination of silicon vacancies and interstitials.

VII. SUMMARY AND CONCLUSION

The microscopic picture of the annealing mechanisms of vacancies and interstitials has been developed from theoretical investigations based on *ab initio* methods within the framework of DFT. We analyzed in detail the ground-state configurations of Frenkel pairs formed by carbon (silicon) vacancies and interstitials and calculated the recombination barriers. We investigated the capture (and emission) of carbon interstitials by (from) carbon interstitial clusters. Various clusters involving up to four carbon interstitials were considered and the energy needed to emit single carbon interstitials from these clusters was calculated.

A hierarchy of annealing mechanisms has been derived that arrange the vacancy-interstitial recombination and the carbon clustering in order with diffusion-based mechanisms and the metastability of the silicon vacancy. The recombination barriers and dissociation energies were compared with the barriers of interstitial and vacancy migration as well as the transformation barrier of the silicon vacancy. The relevance of the Fermi-level effect was demonstrated for the annealing hierarchy of the silicon vacancy and interstitial. The effect originates from two distinct configurations of the silicon interstitial in *p*-type and compensated (or *n*-type) material and the stabilization of the silicon vacancy in *n*-type material. In both cases a strong variation of the migration and transformation barriers with the Fermi level is observed, which changes the hierarchical ordering of the annealing mechanisms. While in compensated material the vacancy-interstitial recombination and the diffusion-based annealing of silicon interstitials are activated at lower temperatures than the metastability-related annealing of the silicon vacancy, this ordering is reversed in *p*-type material. In *n*-type material the metastability-based annealing is unavailable and a diffusion-based mechanism is observed instead. Regarding the annealing of carbon interstitials and vacancies, the highly mobile carbon interstitials were shown to drive the vacancy-interstitial recombination and the formation of thermally stable carbon-interstitial clusters at the early stage of the annealing. The comparably low mobility of the carbon vacancy permits its diffusion-based annealing only at elevated temperatures. In this case, the hierarchical ordering was found to be independent of the Fermi-level effect. The emission of

carbon interstitials from carbon interstitial clusters is associated with activation energies that exceed the activation energies of the vacancy migration. Thus the clusters can provide carbon interstitials even at temperatures at which isolated carbon vacancies have vanished.

The annealing hierarchy was discussed in the light of annealing experiments on EPR and PAS centers, supported by the recent microscopic identification of these centers through experimental and theoretical analysis. A consistent interpretation of the present experimental data for 3C-SiC is facilitated by the proposed annealing hierarchy. The available experiments and theoretical work for 4H-SiC and 6H-SiC suggest that our qualitative conclusions should (with some limitations) apply to other polytypes. With the present analysis we hope to stimulate further experimental investigation of the defects' annealing kinetics. In particular, the annealing stages of the silicon vacancy above 1000 °C and the confirmation of the tentative assignment of the EPR centers $T5$, $EI1$, and $EI2$ to carbon interstitials call for further clarification. Also the role of defect aggregates, as exemplified by carbon interstitials, needs an experimental substantiation. These aggregates should provide a missing link between the kinetics of the primary defects and the thermally stable PL centers.

ACKNOWLEDGMENTS

Fruitful discussions with G. Pensl, W. J. Choyke, M. E. Zvanut, and N. T. Son are gratefully acknowledged. This work was supported by the Deutsche Forschungsgemeinschaft within the SiC Research Group.

[1] W.J. Choyke and L. Patrick, Phys. Rev. B **4**, 1843 (1971).
[2] L. Patrick and W.J. Choyke, Phys. Rev. B **5**, 3253 (1972).
[3] T. Egilsson, J.P. Bergman, I.G. Ivanov, A. Henry, and E. Janzén, Phys. Rev. B **59**, 1956 (1999).
[4] L. Patrick and W.J. Choyke, J. Phys. Chem. Solids **34**, 565 (1973).
[5] S.G. Sridhara, D.G. Nizhner, R.P. Devaty, W.J. Choyke, T. Dalibor, G. Pensl, and T. Kimoto, Mater. Sci. Forum **264-268**, 495 (1998).
[6] A. Kawasuso, F. Redmann, R. Krause-Rehberg, T. Frank, M. Weidner, G. Pensl, P. Sperr, and H. Itoh, J. Appl. Phys. **90**, 3377 (2001).
[7] G.A. Evans, J.W. Steeds, L. Ley, M. Hundhausen, N. Schulze, and G. Pensl, Phys. Rev. B **66**, 035204 (2002).
[8] J.A. Freitas, G. Bishop, J.A. Edmond, J. Ryu, and R.F. Davis, J. Appl. Phys. **61**, 2011 (1987).
[9] T. Egilsson, A. Henry, I.G. Ivanov, J.L. Lindström, and E. Janzén, Phys. Rev. B **59**, 8008 (1999).
[10] A. Kawasuso, H. Itoh, S. Okada, and H. Okumura, J. Appl. Phys. **80**, 5639 (1996).
[11] G. Brauer, W. Anwand, P.G. Coleman, A.P. Knights, F. Plazaola, Y. Pacaud, W. Skorupa, J. Störmer, and P. Willutzki, Phys. Rev. B **54**, 3084 (1996).
[12] A. Kawasuso, H. Itoh, N. Morishita, M. Yoshikawa, T. Ohshima, I. Nashiyama, S. Okada, H. Okumura, and S. Yoshida, and T. Ohshima, Appl. Phys. A: Mater. Sci. Process. **67**, 209 (1998).
[13] A. Polity, S. Huth, and M. Lausmann, Phys. Rev. B **59**, 10 603 (1999).
[14] H. Itoh, A. Kawasuso, T. Ohshima, M. Yoshikawa, I. Nashiyama, S. Tanigawa, S. Misawa, H. Okumura, and S. Yoshida, Phys. Status Solidi A **162**, 173 (1997).
[15] T. Wimbauer, B.K. Meyer, A. Hofstaetter, A. Scharmann, and H. Overhof, Phys. Rev. B **56**, 7384 (1997).
[16] H.J. von Bardeleben, J.L. Cantin, L. Henry, and M.F. Barthe, Phys. Rev. B **62**, 10 841 (2000).
[17] N.T. Son, P.N. Hai, and E. Janzén, Phys. Rev. B **63**, 201201 (2001); T. Umeda, J. Isoya, N. Morishita, T. Oshima, and T. Kamiya, *ibid.* **69**, 121201 (2004).
[18] G. Brauer, W. Anwand, E.-M. Nicht, J. Kuriplach, M. Sob, N. Wagner, P.G. Coleman, M.J. Puska, and T. Korhonen, Phys. Rev. B **54**, 2512 (1996).
[19] T.E.M. Staab, L.M. Torpo, M.J. Puska, and R.M. Nieminen, Mater. Sci. Forum **353-356**, 533 (2001).
[20] V.V. Konovalov, M.E. Zvanut, V.F. Tsvetkov, J.R. Jenny, S.G. Müller, and H.M. Hobsgood, Physica B **308-310**, 671 (2001).
[21] V.Y. Bratus, I.N. Makeeva, S.M. Okulov, T.L. Petrenko, T.T. Petrenko, and H. von Bardeleben, Physica B **309-310**, 621 (2001).
[22] T.T. Petrenko, T.L. Petrenko, V.Y. Bratus, and J.L. Monge, Physica B **308-310**, 637 (2001).
[23] M. Bockstedte, M. Heid, A. Mattausch, and O. Pankratov, Mater. Sci. Forum **389-393**, 471 (2002).
[24] M. Bockstedte, M. Heid, and O. Pankratov, Phys. Rev. B **67**, 193102 (2003).
[25] A. Kawasuso, H. Itoh, T. Ohshima, K. Abe, and S. Okada, J. Appl. Phys. **82**, 3232 (1997).
[26] T. Lingner, S. Greulich-Weber, J.-M. Spaeth, U. Gerstmann, E. Rauls, Z. Hajnal, T. Frauenheim, and H. Overhof, Phys. Rev. B **64**, 245212 (2001).
[27] N.T. Son, E. Sörman, W.M. Chen, C. Hallin, O. Kordina, B. Monemar, E. Janzén, and J.L. Lindstrom, Phys. Rev. B **55**, 2863 (1997).
[28] E. Rauls, T. Lingner, Z. Hajnal, S. Greulich-Weber, T. Frauenheim, and J.-M. Spaeth, Phys. Status Solidi B **217**, R1 (2000).
[29] M. Bockstedte and O. Pankratov, Mater. Sci. Forum **338-342**, 949 (2000).
[30] M. Bockstedte, A. Mattausch, and O. Pankratov, Phys. Rev. B **68**, 205201 (2003).
[31] N. Son, B. Magnusson, Z. Zolnai, A. Ellison, and E. Janzén, Mater. Sci. Forum **433-436**, 45 (2003).
[32] M. Bockstedte, A. Kley, J. Neugebauer, and M. Scheffler, Comput. Phys. Commun. **200**, 107 (1997).
[33] P. Hohenberg and W. Kohn, Phys. Rev. **136**, B864 (1964).
[34] W. Kohn and J.L. Sham, Phys. Rev. **140**, A1133 (1965).
[35] J.P. Perdew and A. Zunger, Phys. Rev. B **23**, 5048 (1981).
[36] D.M. Ceperley and B.J. Alder, Phys. Rev. Lett. **45**, 566 (1980).
[37] H.J. Monkhorst and J.D. Pack, Phys. Rev. B **13**, 5188 (1976).
[38] G. Makov and M.C. Payne, Phys. Rev. B **51**, 4014 (1995).

[39] M. Fuchs and M. Scheffler, Comput. Phys. Commun. **119**, 67 (1999).
[40] I.V. Ionova and E.A. Carter, J. Chem. Phys. **98**, 6377 (1993).
[41] A. Zywietz, J. Furthmüller, and F. Bechstedt, Phys. Rev. B **59**, 15 166 (1999).
[42] L. Torpo, M. Marlo, T.E.M. Staab, and R.M. Nieminen, J. Phys.: Condens. Matter **13**, 6203 (2001).
[43] E. Rauls, T.E.M. Staab, Z. Hajnal, and T. Frauenheim, Physica B **308-310**, 645 (2001).
[44] F. Gao and W.J. Weber, J. Appl. Phys. **94**, 4348 (2003).
[45] L. Torpo, T.E.M. Staab, and R.M. Nieminen, Phys. Rev. B **65**, 085202 (2002).
[46] J.P. Goss, B.J. Coomer, R. Jones, T.D. Shaw, P.R. Briddon, M. Rayson, and S. Öberg, Phys. Rev. B **63**, 195208 (2001).
[47] A. Gali, P. Deák, P. Ordejón, N.T. Son, E. Janzén, and W.J. Choyke, Phys. Rev. B **68**, 125201 (2003).
[48] A. Mattausch, M. Bockstedte, and O. Pankratov, Phys. Rev. B **69**, 045322 (2004).
[49] A. Mattausch, M. Bockstedte, and O. Pankratov (unpublished).
[50] A. Mattausch, M. Bockstedte, and O. Pankratov, Mater. Sci. Forum **353-356**, 323 (2001).
[51] J. Bourgoin and M. Lannoo, *Point Defects in Semiconductors II*, *Springer Series in Solid-State Sciences*, Vol. 35 (Springer-Verlag, Berlin, 1983).
[52] H. Itoh, N. Hayakawa, I. Nashiyama, and E. Sakuma, J. Appl. Phys. **66**, 4529 (1989).
[53] V.S. Vainer and V.A. Il'in, Sov. Phys. Solid State **23**, 2126 (1981).
[54] U. Gerstmann, E. Rauls, T. Frauenheim, and H. Overhof, Phys. Rev. B **67**, 205202 (2003).
[55] V.S. Vainer and V.A. Il'in, Sov. Phys. Solid State **23**, 1432 (1981).
[56] A. Kawasuso (private communication).
[57] M.J. Puska and R.M. Nieminen, Rev. Mod. Phys. **66**, 841 (1994).
[58] B. Aradi, A. Gali, P. Deák, J.E. Lowther, N.T. Son, E. Janzén, and W.J. Choyke, Phys. Rev. B **63**, 245202 (2001).
[59] A. Gali, B. Aradi, P. Deák, W.J. Choyke, and N.T. Son, Phys. Rev. Lett. **84**, 4926 (2000).
[60] T.T. Petrenko, T.L. Petrenko, and V.Y. Bratus, J. Phys.: Condens. Matter **14**, 12 433 (2002).
[61] A. Gali, P. Deák, N.T. Son, E. Janzén, H.J. von Bardeleben, and J.-L. Monge, Mater. Sci. Forum **433-436**, 511 (2003).
[62] T.A.G. Eberlein, C.J. Fall, R. Jones, P.R. Briddon, and S. Öberg, Phys. Rev. B **65**, 184108 (2002).
[63] A. Gali, P. Deák, E. Rauls, N.T. Son, I.G. Ivanov, F.H.C. Carlsson, E. Janzén, and W.J. Choyke, Phys. Rev. B **67**, 155203 (2003).
[64] A. Mattausch, M. Bockstedte, and O. Pankratov, Physica B **308-310**, 656 (2001).
[65] D.J. Eaglesham, P.A. Stolk, H.-J. Gossmann, and J.M. Poate, Appl. Phys. Lett. **65**, 2305 (1994).
[66] N.T. Son, P.N. Hai, and E. Janzén, Mater. Sci. Forum **353-356**, 499 (2001).
[67] M. Bockstedte, M. Heid, A. Mattausch, and O. Pankratov, Mater. Sci. Forum **433-436**, 471 (2003).
[68] M.E. Zvanut and V.V. Konovalov, Appl. Phys. Lett. **80**, 410 (2002).
[69] N.T. Son, B. Magnusson, and E. Janzén, Appl. Phys. Lett. **81**, 3945 (2002).
[70] Y. Zhang, W.J. Weber, W. Jiang, A. Hallén, and G. Possnert, J. Appl. Phys. **91**, 6388 (2002).
[71] A.Y. Kuznetsov, J. Wong-Leung, A. Hallén, C. Jagadish, and B.G. Svensson, J. Appl. Phys. **94**, 7112 (2003).